X-ray diffraction imaging of strain fields in a domain-inverted $LiTaO_3$ crystal

Kh. Hassani,[1] M. Sutton,[2,a)] M. Holt,[3] Y. Zuo,[4] and D. Plant[4]
[1]*Physics Department, University of Tehran, North Kargar Ave., P.O. Box, 14395-547 Tehran, Iran*
[2]*Physics Department, McGill University, Montréal, Quebec H3A 2T8, Canada*
[3]*X-ray Imaging Group, Center for Nanoscale Materials, Argonne National Laboratory, Argonne Illinois 60439 USA*
[4]*Electrical and Computer Engineering, McGill University, Montréal, Quebec H3A 2T8, Canada*

(Received 22 February 2008; accepted 12 June 2008; published online 22 August 2008)

We investigate lattice orientation and strain fields across ferroelectric domain walls in a single crystal lithium tantalate using x-ray diffraction imaging (topography). The sample is an actual voltage-operated optical switch consisting of a series of triangular polarization-inverted domains formed in an originally poled single crystal. By applying an electric field only about 2% of the coercive field in the forward and reverse directions, we observed asymmetric lattice rotation of about 10^{-6} rad, and normal strain variation in the order of 10^{-5} with reference to the zero-field state. Our results confirm that in congruent $LiTaO_3$ crystals there is unexpectedly large strain field expanding several micrometers across the domain walls, in contrast with the widely accepted theoretical fact that in this material the polarization reversal establishes over only a few lattice constants, resulting in small and localized lattice distortions. © *2008 American Institute of Physics*. [DOI: 10.1063/1.2968224]

I. INTRODUCTION

Ferroelectric crystals have many novel applications in science and technology, including nonvolatile random access memories (NVRAMs),[1,2] electro-optic devices,[3–6] and microsensors and actuators.[7] $LiTaO_3$ and $LiNbO_3$ are transparent to light and have high electro-optic and nonlinear optical constants. In addition, their relatively simple 180° domain structure, facilitates engineering the domains in various shapes and sizes to match the requirements for the desired optical devices.[8–11] In these crystals lattice polarization is a result of rearrangement of the positive and negative ions and, therefore, is coupled to lattice strain. First principle calculations[12] have predicted that 180° domain walls in $LiTaO_3$ and $LiNbO_3$ must be atomistically sharp. However, many experiments[13,14] have provided strong evidence that in these crystals the strain field extends several micrometers around 180° walls. This would imply that the strain gradient across the domain walls does not exactly follow the polarization gradient. Deviation from stoichiometry and defects are mainly believed to be responsible for this deviation.[15,16] Since macroscopic properties such as electro-optic constant, switching time, voltage, and index of refraction of devices based on ferroelectric crystals are governed by their microstructure,[17,18] a detailed understanding of the microscopic characteristics of these materials is a key to improve their various applications.

The variety of techniques, such as near-field scanning optical microscopy,[19,20] piezoelectric force microscopy,[6] optical imaging,[21] scanning electron microscopy,[22,23] transmission electron microscopy,[24,25] and high resolution x-ray diffraction[26,27] used to study the microstructure of ferroelectric domain walls, indicates the amount of interest and work dedicated to this subject. X-ray diffraction imaging[28–30] (XDI) is well suited for high spatial resolution measurements of the microstructure in crystals. It has been successfully used by many authors[14,31–33] to investigate different properties of ferroelectric domains. In this work, we present the results of our XDI study of lattice rotation and strain fields around 180° domain walls in a $LiTaO_3$ single crystal. The sample is an electro-optic beam deflector based on the change in the index of refraction in a series of antiparallel ferroelectric domains when applying an electric field.[34] We measured the two-dimensional maps of the strain field and lattice rotation for zero field, as well as when an electric field only about 2% of the coercive field is applied parallel or opposite to the direction of the polarization in the originally poled crystal.[35] This was to study the effect of applied electric field during the use of this device on the microstructure of the domains and domain walls. In agreement with previous studies[14,31] we observed strain in the order of 2×10^{-5} near the domain walls in the zero-field state which extends several micrometers around the walls. We provide convincing evidence that the lattice rotation and strain enhancement by applying an electric field in the order of ±420 kV/m, depend on the wall orientation with respect to the crystal lattice and the direction of the electric field due to the presence of an internal electric field.[35,36]

In Secs. II and IV, our experimental setup will be reviewed and the method of analysis will be described. Results will be given for the strain and lattice rotations fields for 0 and ±210 V. Finally, their implications are discussed.

II. EXPERIMENT

The measurements were done at the 8-ID-E side section of IMM/XOR-CAT (IBM, MIT, and McGill X-ray Operations and Research Collaborative Access Team) at the Ad-

a)Author to whom correspondence should be addressed. Electronic mail: mark@physics.mcgill.ca.

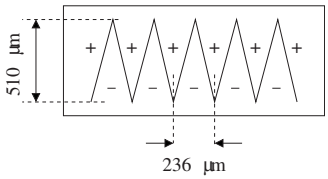

FIG. 1. 180° domain structure in the electro-optical switch: triangle-shaped antiparallel domains are created by domain inverting an originally poled $LiTaO_3$ single crystal.

vanced Photon Source, Argonne National Laboratory. Our sample was a 0.5 mm thick $LiTaO_3$ single crystal composed of antiparallel domains formed by inverting the polarization of triangular regions (Fig. 1) in an originally poled crystal by applying a pulsed electric field bigger than the coercive field of the crystal. This sample was designed and made to be used as an electro-optics switch.[34] Gold electrodes were deposited on both sides of the sample to apply an electric field to the domains. We used the same XDI setup as in our previous study[37] duplicated in Fig. 2. Parallel 7.5 keV x rays from the synchrotron source were filtered by a Si(022) monochromator and illuminated the crystal which was mounted on a high resolution four-axes diffractometer. We employed a Si(111) channel-cut analyzer[38] to resolve the diffraction angle 2θ, and a charge coupled device (CCD) camera microscopically imaging a fluorescent screen, resulting in 0.7×0.7 μm^2 pixel size for the x-ray images. Several mesh scans of size 80×40 [analyzer (θ_{anal}) $\times$ sample (θ)] with 3×10^{-4} and 5×10^{-4} deg step sizes about the (006) Bragg peak angles were done and at each position the diffracted rays were recorded. This process generates a four-dimensional $(2\theta, \theta, x, y)$ data array which is then digitally restacked to correct for the lateral drift of the image on the detector screen caused by the analyzer scan. Scans were repeated with a ± 210 V applied to the crystal electrodes. This is about 2% of the coercive field (21 MV/m) of the congruent $LiTaO_3$ crystals.[13]

The resolution of this setup has several aspects. The θ and 2θ resolutions are better than 0.0005° full width at half maximum (FWHM). Peak positions can be measured to a fraction of this (at least 10%). This leads to a resolution in strain of at least ppm. The spatial resolution of our imaging CCD setup has been measured to be better than 3 μm FWHM.[37]

III. ANALYSIS AND RESULTS

The restacked data provide two-dimensional (2D) θ-2θ Bragg peak patterns for every (x, y) point of the sample. The

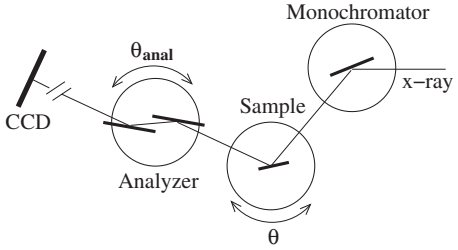

FIG. 2. Experiment setup: analyzer and sample mesh scans generate four-dimensional stack of images.

important advantage of using the channel-cut analyzer should be emphasized here. It allows us to unambiguously distinguish a small lattice rotation from a lattice strain which might, otherwise, be misinterpreted.

The most obvious way to analyze the data, is to fit a peak shape to each θ-2θ peak. Although not perfect, the data were fit to 2D Gaussian peaks. This gives results for intensity, peak rotation, and strain at each point for all three values of voltage. The 2D Gaussian fits have rather noisy fit parameters but have the advantage of giving absolute peak properties. Figure 3(a) shows a typical fit and also why fitting to any simple peak shape leads to problems. To better quantify the effect of the applied voltages on the Bragg peaks, we developed a custom fitting scheme. The peak shifts in the θ and 2θ directions and the intensity change with respect to the zero-field peak were determined by fitting to a "scaled and shifted pattern" interpolated from the zero-field data. When this procedure results in good fits, as it does here, it has several advantages. There is no need to use a complicated analytical fit function for the peaks and it reduces systematic error. Any large changes in line shape are identifiable as the quality of the fit (chi-square value) deteriorates. Moreover, small changes from extraneous features in the data due to surface morphology and backgrounds are considerably eliminated. For these data, the fit results provide us with high quality 2D maps of relative changes in the lattice orientation θ and strain field (from 2θ map) as a result of the applied voltages. Figures 3(a) and 3(b) compare the two fit methods for a typical point on the sample.

Statistical errors in our peak fitting methods for the rotation angle and strain were about 10% for the Gaussian fits and less than 2% for the custom fits. However, there are systematic errors arising from the oversimplified peak shape for the Gaussian fits and from any variations in the reference for the custom method.

Lattice rotation is obtained directly from the sample angle, θ. Strain maps can be easily calculated from the 2θ maps using the derivative of Bragg's law:

$$\frac{\delta(d)}{d} = -\cot\left(\frac{2\theta}{2}\right)\delta\left(\frac{2\theta}{2}\right). \quad (1)$$

2D maps of the relative (with reference to the zero-field) lattice reorientation and strain under ± 210 V voltages are shown in Figs. 4 and 5, respectively.

Cross sections of these graphs averaged over 150 pixels (~ 96 μm) in the y direction for a selected region are plotted in Fig. 6.

IV. INTERPRETATION OF THE RESULTS

The first obvious feature of all the strain graphs is that the strain field extends about 50 μm around the domain walls. Theoretical calculations[12] predict the polarization gradient across a 180° domain wall in $LiTaO_3$ to be atomistically sharp (a few lattice constants wide). Since there is no lattice mismatch across an ideal 180° wall, one would expect to see small strain only in the region where polarization switching occurs. However, our results confirm the previous experimental studies[13,39] arguing that in congruent $LiTaO_3$

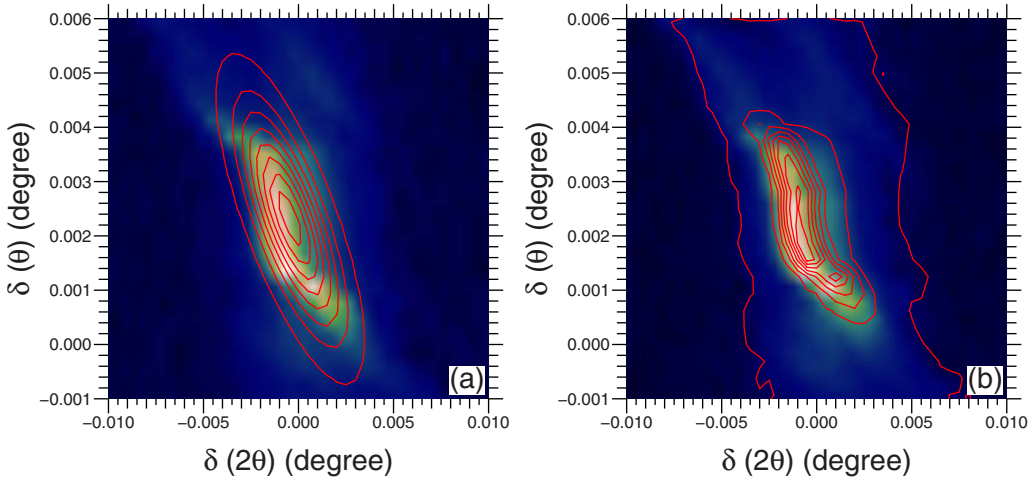

FIG. 3. (Color online) Examples of the θ-2θ peak fits. This peak corresponds to position (570, 220 μm) of the 210 V sample in Figs. 4 and 5. (a) 2D Gaussian peak fit, red lines are contours from the fit superimposed on the data. (b) Custom fit, red lines are contours from the shifted and scaled peak at 0 V.

crystals, because of nonstoichiometry defects, unexpectedly large strain gradients extend far beyond the domain wall. As can be seen from the absolute fit graphs [Fig. 6(b)], strain as big as 2×10^{-5} is present near the domain walls even without applying any voltage, which could be a result of local defects and polarized domain walls (see below). The strain around 180° domain walls here is almost the same size as observed in our previous study[40] for the 90° domains in $BaTiO_3$. The piezoelectric constant for $LiTaO_3$ is 8.8 pm/V (Ref. 41) giving a strain of 6×10^{-6} for a 180° domain wall at 210 V.

Figures 4 and 5, and the corresponding one-dimensional graphs, show that negative voltages induce a bigger effect on both the lattice rotation and the strain. This is most likely related to an internal electric field[35,36] parallel to the polarization direction of the originally poled crystal which favors one direction more than the other.

The next interesting aspect, seen in Figs. 6(a) and 6(c), is the highly asymmetric behavior of the lattice rotation near opposite domain walls. For the odd-numbered walls, applying a negative voltage causes almost no rotation, but a positive voltage induces a lattice rotation as big as -6×10^{-4} deg. For the even-numbered walls, however, the results of the two voltages are only slightly different. Strain is coupled to the lattice rotation and shows a range of 0 down to -2×10^{-5} which also switches between even and odd domain walls as the electric field does. These imply that the domain walls in our sample are not neutral, and possess different states of polarization. The odd-numbered walls being highly polarized parallel to the internal electric field, favor the negative field by responding with almost no rotation and strain, and a large rotation and strain to the positive field. The even-numbered walls, on the other hand, have a smaller polarization antiparallel to the internal field and, therefore, the effect is less profound and in the opposite direction. As Fig. 7 demonstrates, the angle between the orientation of the odd and even walls (imposed by the electrodes used to poll the sample) and the natural domain wall orientation in this crystal [(110)

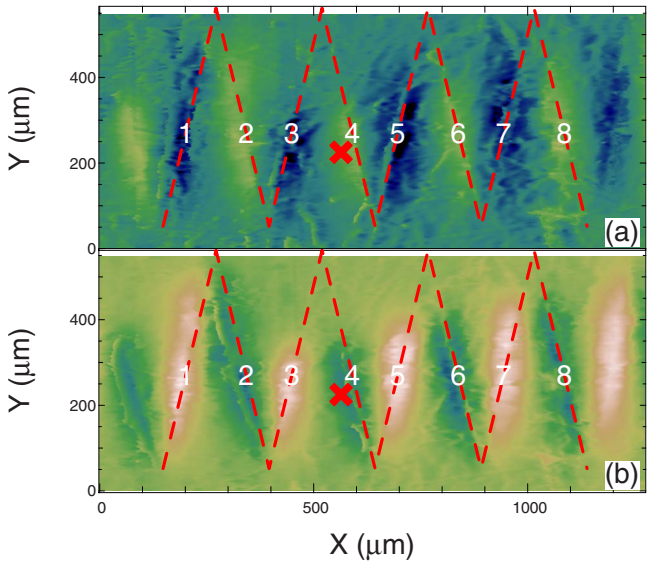

FIG. 4. (Color online) Lattice rotation maps: (a) 210 V and (b) −210 V. Dashed lines (red) show the domain walls as initially polled.

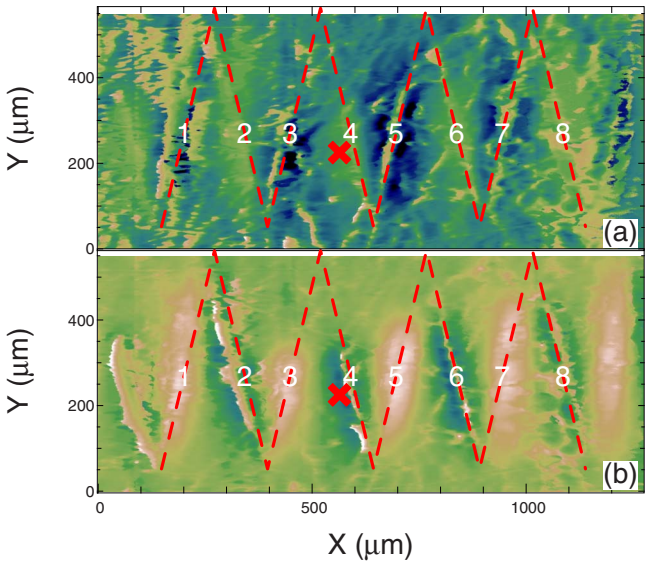

FIG. 5. (Color online) Strain maps: (a) 210 V and (b) −210 V.

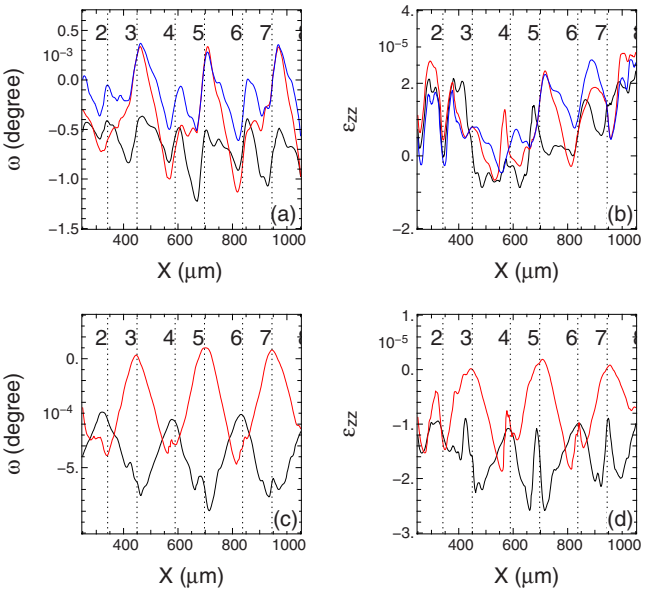

FIG. 6. (Color online) [(a) and (b)] Lattice rotation and strain for the 210 V (black), −210 V (red), and zero (blue) voltages calculated by the Gaussian fit method. [(c) and (d)] Same quantities from the custom fit method. Dotted lines indicate the intersection with the domain walls.

planes] are different. We expect this to be the origin of the different nonzero polarization states of the two types of the walls.

More detailed information can be inferred by a closer look at Fig. 6(d). Interestingly, the rotation and the strain are proportional to each other (except for the sharp features at the minima). A change in surface height is proportional to the change in strain. If the rotation resulted simply from a change in height, it would be proportional to the slope of the height profile and not the height. To reiterate, for our 0.5 mm thick crystal a strain of 1×10^{-5} leads to a height change of 5 nm. At the midpoint of the triangle (100 μm wide) this would give an angle of 0.003°, which is bigger than what we observe.

Also, the curves exhibit relatively sharp local maxima at the bottom of their minima, occurring at the odd walls for positive field, and the even walls for negative fields. We attribute these sharp maxima to the local polarization gradient across the domain walls causing a rapid change in the strain profile.

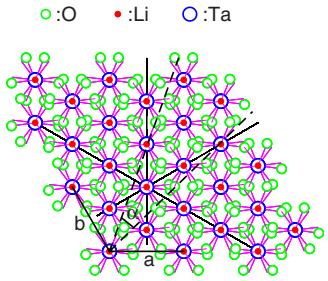

FIG. 7. (Color online) Orientation of the domain walls (dashed lines) imposed by the triangle-shaped electrodes with respect to the natural domain walls [(110) planes shown with solid lines], and atoms in the lattice with respect to the crystal. Domain walls make angles of 10.5° and 15.5° with respect to [110] (α=26°).

V. SUMMARY

In this work we have investigated the lattice rotation and strain field around antiparallel 180° domain walls in a single crystal $LiTaO_3$ sample using high resolution XDI. We studied the crystal in the zero-field state and for an electric field as small as 2% of the coercive field of the material applied in the two polarization directions. We found a strain of order 2×10^{-5} around the domain walls in the zero-field state. Our study confirms the previously established fact that in congruent $LiTaO_3$ crystals strain field larger than what is expected for a 180° wall expands several micrometers around the domain walls. The sample in our study had two groups of domain walls with slightly different orientations with respect to the crystal axes. Our experiment shows asymmetric lattice rotation reaching a maximum of -6×10^{-4} deg, and a corresponding strain field in the order of -2×10^{-5} around the two types of the domain walls. We associate the observed asymmetry to the presence of the internal electric field and differently polarized domain walls. We were also able to measure a signature of the sharp polarization gradient across the domain walls in the measured strain profile.

The sample used in this work was originally designed as an electro-optic switch. If the observed strain patterns persist to the much higher voltages used by the device, the domain walls will induce gradients in the index of refraction and affect the calculation of angles for designing the switch. Optimizing the alignment of the domain walls used in the switch should lead to improved switching behavior.

Finally, we would like to stress the power of XDI with appropriate data analysis. It provides a powerful tool to measure and understand microstructure in crystalline material and is relatively underutilized.

ACKNOWLEDGMENTS

Use of the Advanced Photon Source was supported by the U.S. Department of Energy, Office of Basic Sciences, under Contract No. W-31–109-Eng-38.

[1] *Ferroelectric Random Access Memories: Fundamentals and Applications*, edited by H. Ishiwara, M. Okuyama, and Y. Arimoto (Springer, New York, 2004).
[2] O. Auciello, J. F. Scott, and R. Ramesh, Phys. Today **51**(7), 22 (1998).
[3] Y. Xu, *Ferroelectric Materials and their Applications* (Elsevier, New York, 1991).
[4] H. Onaka, 30th European Conference on Optical Communication, ECOC 2004, Stockholm, Sweden, 2004 (unpublished), Vol. 2, pp. 280–1.
[5] S. Liu and X. Min, Appl. Phys. Lett. **88**, 143512 (2006).
[6] D. Scrymgeour and V. Gopalan, Phys. Rev. B **72**, 024103 (2005).
[7] P. Muralt, J. Micromech. Microeng. **10**, 136 (2000).
[8] V. Shur, E. Rumyantsev, E. Nikolaeva, E. Shishkin, R. Batchko, M. Fejer, and R. Byer, Ferroelectrics **257**, 191 (2001).
[9] V. Shur, E. Rumyantsev, E. Nikolaeva, E. Shishkin, R. Batchko, G. Miller, M. Fejer, and R. Byer, Proc. SPIE **3992**, 143 (2000).
[10] V. Shur, E. Rumyantsev, R. Batchko, G. Miller, M. Fejer, and R. Byer, Ferroelectrics **221**, 157 (1999).
[11] V. Shur, Ferroelectrics **340**, 3 (2006).
[12] J. Padilla, W. Zhong, and D. Vanderbilt, Phys. Rev. B **53**, R5969 (1996).
[13] S. Kim, V. Gopalan, K. Kitamura, and Y. Furukawa, J. Appl. Phys. **90**, 2949 (2001).
[14] T. Jach, S. Kim, V. Gopalan, S. Durbin, and D. Bright, Phys. Rev. B **69**, 064113 (2004).
[15] S. Kim, B. Steiner, A. Gruverman, and V. Gopalan, AIP Conf. Proc. **626**, 277 (2002).

[16]V. Gopalan, K. Kitamura, and Y. Furukawa, AIP Conf. Proc. **535**, 183 (2000).
[17]L. Tian and V. Gopalan, Proc. SPIE **5728**, 278 (2005).
[18]K. Kitamura, Y. Furukawa, K. Niwa, V. Gopalan, and T. Mitchell, Appl. Phys. Lett. **73**, 3073 (1998).
[19]T. Yang, V. Gopalan, P. Swart, and U. Mohideen, J. Phys. Chem. Solids **61**, 275 (2000).
[20]S. Kim and V. Gopalan, Mater. Sci. Eng., B **120**, 91 (2005).
[21]L. Tian, D. Scrymgeour, and V. Gopalan, J. Appl. Phys. **97**, 114111 (2005).
[22]S. Zhu and W. Cao, Phys. Status Solidi A **173**, 495 (1999).
[23]U. Lev, E. Zolotoyabko, D. Towner, A. Meier, and B. Wessels, J. Phys. D **38**, A184 (2005).
[24]E. Snoeck, L. Normand, A. Thorel, and C. Roucau, Phase Transitions **46**, 77 (1994).
[25]S. I. Yakunin, V. V. Shakamanov, G. V. Spivak, and N. V. Vasil'eva, Sov. Phys. Solid State **14**, 310 (1972).
[26]H. Evans Jr., Acta Crystallogr. **14**, 1019 (1961).
[27]E. Zolotoyabko, J. P. Quintana, B. H. Hoerman, and B. W. Wessels, Appl. Phys. Lett. **80**, 3159 (2002).
[28]A. Authier, *Dynamical Theory of X-Ray Diffraction* (Oxford University, New York, 2001).
[29]D. K. Bowen and B. K. Tanner, *High Resolution X-Ray Diffractometery and Topography* (Taylor & Francis, London, 1998).
[30]P. F. Fewster, J. Appl. Crystallogr. **24**, 178 (1991).
[31]S. Kim, V. Gopalan, and B. Steiner, Appl. Phys. Lett. **77**, 2051 (2000).
[32]M. Drakopoulos, Z. W. Hu, S. Kuznetsov, A. Snigirev, I. Snigireva, and P. A. Thomas, J. Phys. D **32**, A160 (1999).
[33]R. C. Rogan, N. Tamura, G. A. Swift, and E. Üstündag, Nat. Mater. **2**, 379 (2003).
[34]Y. Zuo, B. Bahamin, E. Tremblay, C. Pulikkaseril, E. Shoukry, M. Mony, P. Langlois, V. Aimez, and D. Plant, IEEE Photonics Technol. Lett. **17**, 2080 (2005).
[35]V. Gopalan and M. Gupta, Appl. Phys. Lett. **68**, 888 (1996).
[36]V. Gopalan and M. Gupta, J. Appl. Phys. **80**, 6099 (1996).
[37]K. Hassani, M. Sutton, A. Tkachuk, and M. Holt, J. Appl. Phys. **101**, 063546 (2007).
[38]R. Khachatryan, A. Tkachuk, Y. S. Chu, J. Qian, and A. Macrander, Proc. SPIE **5537**, 171 (2004).
[39]S. Kim, V. Gopalan, and A. Gruverman, Appl. Phys. Lett. **80**, 2740 (2002).
[40]M. Holt, K. Hassani, and M. Sutton, Phys. Rev. Lett. **95**, 085504 (2005).
[41]D. Royer and V. Kmetik, Electron. Lett. **28**, 1828 (1992).